

Magnetohydrodynamic flow in a curved pipe

F. Issacci, N. M. Ghoniem, and I. Catton

Mechanical, Aerospace, and Nuclear Engineering Department, University of California at Los Angeles, Los Angeles, California 90024

(Received 24 June 1987; accepted 22 September 1987)

The flow of conductive fluids in highly conductive curved pipes is studied analytically in this paper. The flow is assumed to be steady state, laminar, and fully developed. Coupled continuity, Navier–Stokes, and appropriate Maxwell equations are solved in toroidal coordinates. The dimensionless parameters of the problem are Dean number K and Hartmann number Ha . For low Hartmann numbers [$Ha^2 \sim \mathcal{O}(1)$], the solution is expanded in a power series of K and Ha^2 . For intermediate Hartmann numbers [$Ha^2 \sim \mathcal{O}(1000)$], the solution is expressed as a power series of K . The axial velocity contours are shown to be shifted toward the outer wall. For low Ha , these contours are nearly circular. The effect of a strong transverse magnetic field is to enhance the compression of fluid toward the outer wall. The secondary flow field comprises a symmetric pair of counter-rotating vortices. A strong magnetic field is found to confine the secondary flow streamlines to a thin layer near the tube wall. The secondary flow rate in the near-wall boundary layer is increased by the magnetic field. This increase in flow rate raises the possibility of efficient convective cooling of curved first wall tubes in magnetic confinement fusion reactors (MFCR).

I. INTRODUCTION

A number of magnetic confinement fusion reactor (MCFR) concepts have been based on the use of liquid lithium or lithium lead for the dual function of tritium breeding and cooling of first wall/blanket structures. In these “self-cooled” concepts, the conducting fluid flows in a strong magnetic field. The applied magnetic field, which is primarily intended for plasma confinement, introduces significant body forces that can drastically influence fluid motion. Because of the nature of plasma confinement in a torus, the fluid can be circulated toroidally or poloidally around the plasma. The result is that we are faced with a conducting fluid flowing in a curved pipe in the presence of an imposed magnetic field. If the imposed magnetic field is parallel to the flow, no magnetic body force arises. However, when the imposed magnetic field is transverse to the flow, the effects of induced magnetic body forces must be considered.¹

A proper understanding of fluid flow in a fusion reactor involves the solution of magnetohydrodynamic (MHD) equations. These equations in fluid flow are basically the fluid continuity, the Navier–Stokes, and the appropriate Maxwell equations. To date no numerical code exists that can solve such MHD equations in three dimensions in their most general form. In complex geometries, two-dimensional numerical solutions² are also difficult. In this paper, we present analytical approximations to the solution of MHD equations in curved pipes. These approximate solutions shed light on fluid motion, and can be used for the benchmarking of more general numerical solutions.

Many fusion blanket designs, especially in tokamaks, have complicated flow patterns and straight or curved duct analysis may not be adequate. However, in tandem mirror or reversed field pinch designs, circular curved ducts have been proposed (e.g., the MARS design in Ref. 3).

Flow in curved pipes with no magnetic field is reviewed

by Berger *et al.*⁴ As early as 1928, Dean⁵ presented an analytical series solution to the fully developed flow of nonconducting fluids in curved pipes of small curvatures. The solution was given in terms of the Dean number K which is defined as the ratio of the square root of the product of the inertia and centrifugal forces to the viscous force. Since centrifugal forces and their interaction with viscous forces induce secondary flows, K is a measure of the magnitude of the secondary flow. The Navier–Stokes equation in curved pipes has been solved numerically by McConalogue and Srivastava⁶ for intermediate Dean numbers, and by Collins and Dennis⁷ for high Dean numbers.

The effects of the magnetic field on fluid flow have been studied primarily for straight pipes.^{8–11} The pressure gradient of the laminar flow regime depends upon three parameters: (1) the ratio of magnetic body force to viscous force (Hartmann number, Ha); (2) the ratio of magnetic body force to inertia force (interaction number, N); and (3) the ratio of the wall to liquid flow conductivity (conductance ratio, ϕ). Shercliff⁸ solved the problem of flow in circular pipes under transverse magnetic fields in an approximate manner for large Hartmann numbers assuming walls of zero and small conductivity. The effect of wall conductivity was also studied by Chang and Lundgren.⁹ Pressure drop in thin-walled circular straight ducts was studied by Holroyd and Walker,¹⁰ neglecting the inertial effects and induced magnetic field. Recently, Walker developed solutions to MHD flow equations by asymptotic analysis for circular straight ducts under strong transverse magnetic fields.¹¹ In the present work we consider the flow of conductive fluids in highly conductive curved pipes with low [$Ha^2 \approx \mathcal{O}(1)$] and intermediate [$Ha^2 \approx \mathcal{O}(1000)$] Hartmann numbers.

II. PROBLEM FORMULATION

Considering steady-state laminar flow in a curved pipe, we introduce the toroidal coordinate system (r', α, θ) shown

in Fig. 1. Here, r' denotes the distance from the center of the circular cross section of the pipe, α the angle between the radius vector and the plane of symmetry, and θ the angular distance of the cross section from the entry of the pipe. The corresponding velocity components are (u', v', w') .

A. Governing equations

The basic equations for steady-state laminar flow are

$$\text{Continuity: } \nabla \cdot \mathbf{v}' = 0,$$

$$\text{Momentum: } (\mathbf{v}' \cdot \nabla) \mathbf{v}' = - (1/\rho) \nabla p' + \nu \nabla^2 \mathbf{v}' + (1/\rho) \mathbf{J}' \times \mathbf{B}',$$

where ρ is the fluid density and ν is its kinematic viscosity. The last term on the right-hand side of the above equation, $\mathbf{J}' \times \mathbf{B}'$, is the body force introduced by the magnetic field. By Ohm's law we have

$$\mathbf{J}' = \sigma_e (\mathbf{E}' + \mathbf{V}' \times \mathbf{B}'), \quad (1)$$

where the convective electric current is neglected and σ_e is the fluid conductivity. The electric field \mathbf{E}' is related to the conductance ratio ϕ as

$$\mathbf{E}' \sim 1/(1 + \phi).$$

For a highly conducting wall, \mathbf{E}' can be assumed to be zero.¹² Neglecting the force introduced by \mathbf{E}' , the magnetic field body force is written as

$$\mathbf{J}' \times \mathbf{B}' = \sigma_e (\mathbf{v}' \times \mathbf{B}' \times \mathbf{B}').$$

Thus the momentum equation is

$$(\mathbf{v}' \cdot \nabla) \mathbf{v}' = (-1/\rho) \nabla p' + \nu \nabla^2 \mathbf{v}' + (\sigma_e/\rho) (\mathbf{v}' \times \mathbf{B}' \times \mathbf{B}').$$

From Maxwell's equations, and using Eq. (1), the induction equation is written as

$$\frac{\partial \mathbf{B}}{\partial t} = \nabla \times (\mathbf{v}' \times \mathbf{B}') - \nabla \times \left[\left(\frac{1}{\sigma_e} \right) \nabla \times \left(\frac{1}{\mu_e} \right) \mathbf{B}' \right]. \quad (2)$$

Since

$$\nabla \times \nabla \times \mathbf{B}' = \nabla (\nabla \cdot \mathbf{B}') - \nabla^2 \mathbf{B}', \quad (3)$$

and

$$\nabla \cdot \mathbf{B}' = 0, \quad (4)$$

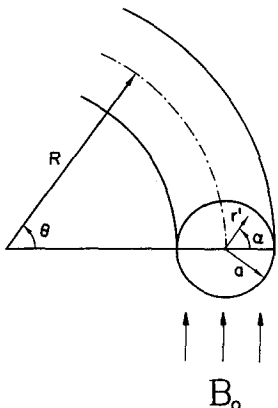


FIG. 1. Toroidal coordinate system (r', α, θ) .

Eqs. (2)–(4) yield, at steady state, the induction equation, which is given by

$$\nabla \times (\mathbf{v}' \times \mathbf{B}') + (1/\sigma_e \mu_e) \nabla^2 \mathbf{B}' = 0.$$

B. Toroidal coordinates

Let us define the following nondimensional variables:

$$r = r'/a, \quad s = R\theta/a, \quad \mathbf{v}(u, v, w) = \mathbf{v}'/\bar{w},$$

$$\delta = a/R, \quad p = p'/(\rho \bar{w}^2), \quad \mathbf{B}(B^r, B^\alpha, B^\theta) = \mathbf{B}'/B_0,$$

where B_0 is the applied transverse magnetic field, \bar{w} is a characteristic average axial flow velocity, and we introduce a scaling transformation as follows:

$$(u, v, w) \rightarrow (\delta u, \delta v, \delta^{-1/2} w),$$

$$(B^r, B^\alpha, B^\theta) \rightarrow (B^r, B^\alpha, \delta^{1/2} B^\theta),$$

$$s = R\theta/a = \delta^{-1/2} z.$$

The scaling transformations of velocities are different from those employed in the work of Berger *et al.*⁴ The motivation behind this specific scaling transformation stems from the coupling of the induction equation and the Navier–Stokes equation. With this scaling, the governing equations [(1)–(4)] take the following form:

$$u_r + u \left(\frac{1 + 2\delta r \cos \alpha}{rh} \right) + \frac{v_\alpha}{r} - \frac{\delta (\sin \alpha) v}{h} + \frac{w_z}{h} = 0, \quad (5)$$

$$\begin{aligned} uu_r + \frac{vu_\alpha}{r} + \frac{wu_z}{h} - \frac{v^2}{r} - \frac{(\cos \alpha) w^2}{h} \\ = -\frac{P_r}{\delta^2} + \frac{1}{\delta \text{Re}} \left[\left(\frac{\delta \sin \alpha}{h} - \frac{1}{r} \frac{\partial}{\partial \alpha} \right) \left(v_r + \frac{v}{r} - \frac{u_\alpha}{r} \right) \right. \\ \left. + \frac{\partial}{\partial z} \left(\frac{\delta u_z}{h^2} - \frac{w_r}{h} - \frac{\delta \cos \alpha}{h^2} w \right) \right] \\ + \frac{\text{Ha}^2}{\delta \text{Re}} [B^\theta (wB^r - \delta uB^\theta) - B^\alpha (uB^\alpha - vB^r)], \end{aligned} \quad (6)$$

$$\begin{aligned} uv_r + \frac{vv_\alpha}{r} + \frac{wv_z}{h} + \frac{uv (\sin \alpha) w^2}{rh} \\ = -\frac{P_\alpha}{\delta^2 r} + \frac{1}{\delta \text{Re}} \left[\left(\frac{\partial}{\partial r} + \frac{\delta \cos \alpha}{h} \right) \left(v_r + \frac{v}{r} - \frac{u_\alpha}{r} \right) \right. \\ \left. + \frac{\partial}{\partial z} \left(\frac{\delta v_z}{h^2} - \frac{w_\alpha}{rh} + \frac{\delta \sin \alpha}{h^2} w \right) \right] \\ + \frac{\text{Ha}^2}{\delta \text{Re}} [B^r (uB^\alpha - vB^r) - B^\theta (\delta vB^\theta - wB^\alpha)], \end{aligned} \quad (7)$$

$$\begin{aligned} ww_r + \frac{vw_\alpha}{r} + \frac{ww_z}{h} + \frac{\delta (\cos \alpha) uw}{h} - \frac{\delta (\sin \alpha) vw}{h} \\ = -\frac{P_z}{\delta h} + \frac{1}{\delta \text{Re}} \left[\left(\frac{\partial}{\partial r} + \frac{1}{r} \right) \left(w_r + \frac{\delta \cos \alpha}{h} w - \frac{\delta u_z}{h} \right) \right. \\ \left. + \frac{\partial}{\partial \alpha} \left(\frac{w_\alpha}{r^2} - \frac{\delta \sin \alpha}{rh} w - \frac{\delta v_z}{rh} \right) \right] \\ + \frac{\text{Ha}^2}{\delta \text{Re}} [B^\alpha (\delta vB^\theta - wB^\alpha) - B^r (wB^r - \delta uB^\theta)], \end{aligned} \quad (8)$$

$$\begin{aligned} & \frac{\delta(\sin \alpha)}{h} (vB^r - uB^\alpha) \\ & + \frac{1}{r} (B^\alpha u_\alpha + uB_\alpha^\alpha - vB_\alpha^r - B^r v_\alpha) \\ & - \frac{1}{h} (B^r w_z + wB_z^r - \delta B^\theta u_z - \delta uB^\theta) \\ & + \frac{1}{\delta \text{Rm}} \left[\frac{\partial}{\partial z} \delta \left(\frac{B_z^r}{h^2} - \frac{\delta(\cos \alpha)B^\theta}{h^2} - \frac{B_r^\theta}{h} \right) \right. \\ & \left. + \left(\frac{\delta \sin \alpha}{h} - \frac{1}{r} \frac{\partial}{\partial \alpha} \right) \left(B_r^\alpha + \frac{B^\alpha}{r} - \frac{B_r^\alpha}{r} \right) \right] = 0, \quad (9) \end{aligned}$$

$$\begin{aligned} & \frac{\delta(\cos \alpha)}{h} (vB^r - uB^\alpha) \\ & + \frac{1}{h} (\delta B^\theta v_z + \delta vB_z^\theta - B^\alpha w_z - wB_z^\alpha) \\ & - (B^\alpha u_r + uB_r^\alpha - B^r v_r - vB_r^\alpha) \\ & + \frac{1}{\delta \text{Rm}} \left[\frac{\partial}{\partial z} \delta \left(\frac{B_z^\alpha}{h^2} + \frac{\delta(\sin \alpha)B^\theta}{h^2} - \frac{B_r^\theta}{rh} \right) \right. \\ & \left. + \left(\frac{\delta \cos \alpha}{h} + \frac{\partial}{\partial r} \right) \left(B_r^\alpha + \frac{B^\alpha}{r} - \frac{B_r^\alpha}{r} \right) \right] = 0, \quad (10) \end{aligned}$$

$$\begin{aligned} & \frac{1}{r} (wB^r - \delta uB^\theta) + (B^r w_r + wB_r^r - \delta B^\theta u_r - \delta uB_r^\theta) \\ & - \frac{1}{r} (\delta B^\theta v_\alpha + \delta vB_\alpha^\theta - B^\alpha w_\alpha - wB_\alpha^\alpha) \\ & + \frac{1}{\text{Rm}} \left[\frac{\partial}{\partial \alpha} \left(\frac{B_\alpha^\theta}{r^2} - \frac{\delta(\sin \alpha)B^\theta}{rh} - \frac{B_z^\alpha}{rh} \right) \right. \\ & \left. + \left(\frac{\partial}{\partial r} + \frac{1}{r} \right) \left(B_r^\theta + \frac{\delta(\cos \alpha)B^\theta}{h} - \frac{B_z^\alpha}{h} \right) \right] = 0, \quad (11) \end{aligned}$$

where $h = 1 + \delta r \cos \alpha$. The subscripts denote derivatives and the nondimensional parameters are defined as $\text{Re} = \bar{w}a/\nu$, $\text{Ha}^2 = \sigma B_0^2 a^2 / (\rho\nu)$, $\text{Rm} = \sigma_e \mu_e \bar{w}a$.

For fully developed flow, the velocity field is independent of z and Eq. (8) shows that the pressure gradient P_z is independent of z . The major component of the pressure P is provided by fluid motion in the axial direction and the secondary flows introduce small contributions to this component. Thus for $\delta \ll 1$ the total pressure may be written as

$$P = P_0(z) + \delta^2 P_1(r, \alpha) + \dots, \quad (12)$$

and $P_0 = -Gz$, where G is a constant.

For the case where the pipe has only slight curvature, i.e., $\delta = a/R \ll 1$, Eqs. (5)–(11) can be rewritten using Eq. (12) as

$$u_r + \frac{u}{r} + \frac{v_\alpha}{r} = 0, \quad (13)$$

$$\begin{aligned} & uu_r + \frac{vu_\alpha}{r} - \frac{v^2}{r} - (\cos \alpha)w^2 \\ & = -\frac{\partial P_1}{\partial r} + \frac{1}{K} \left[-\frac{1}{r} \frac{\partial}{\partial \alpha} \left(v_r + \frac{v}{r} - \frac{u_\alpha}{r} \right) \right] \\ & + \frac{\text{Ha}^2}{K} (wB^r B^\theta - uB^\alpha B^\alpha + vB^r B^\alpha), \quad (14) \end{aligned}$$

$$\begin{aligned} & uv_r + \frac{vv_\alpha}{r} + \frac{uv}{r} + (\sin \alpha)w^2 \\ & = -\frac{1}{r} \frac{\partial P_1}{\partial \alpha} + \frac{1}{K} \left[\frac{\partial}{\partial r} \left(v_r + \frac{v}{r} - \frac{u_\alpha}{r} \right) \right] \\ & + \frac{\text{Ha}^2}{K} (uB^r B^\alpha - vB^r B^r + B^\alpha B^\theta), \quad (15) \end{aligned}$$

$$\begin{aligned} & uw_r + \frac{vw_\alpha}{r} \\ & = -\frac{1}{\delta} \frac{\partial P_0}{\partial z} + \frac{1}{K} \left[\left(\frac{1}{r^2} \right) w_{\alpha\alpha} + \left(\frac{\partial}{\partial r} + \frac{1}{r} \right) w_r \right] \\ & + \frac{\text{Ha}^2}{K} [-w(B^\alpha B^\alpha + B^r B^r)], \quad (16) \end{aligned}$$

$$\begin{aligned} & \frac{1}{r} (B^\alpha u_\alpha + uB_\alpha^\alpha - vB_\alpha^r - B^r v_\alpha) \\ & + \frac{1}{\delta \text{Rm}} \left[-\frac{1}{r} \frac{\partial}{\partial \alpha} \left(B_r^\alpha + \frac{B^\alpha}{r} - \frac{B_r^\alpha}{r} \right) \right] = 0, \quad (17) \end{aligned}$$

$$\begin{aligned} & - (B^\alpha u_r + uB_r^\alpha - vB_r^r - B^r v_r) \\ & + \frac{1}{\delta \text{Rm}} \left[\frac{\partial}{\partial r} \left(B_r^\alpha + \frac{B^\alpha}{r} - \frac{B_r^\alpha}{r} \right) \right] = 0, \quad (18) \end{aligned}$$

$$\begin{aligned} & \frac{w}{r} B^r + B^r w_r + wB_r^r + \frac{1}{r} (B^\alpha w_\alpha + wB_\alpha^\alpha) \\ & + \frac{1}{\text{Rm}} \left[\frac{B_{\alpha\alpha}^\theta}{r^2} + \left(\frac{\partial}{\partial r} + \frac{1}{r} \right) B_r^\theta \right] = 0, \quad (19) \end{aligned}$$

where K , the Dean number, is defined as

$$K = \delta \text{Re} = (a/R)(\bar{w}a/\nu).$$

This definition of the Dean number is different from that of Ref. 4 because of the different scaling transformation. The boundary conditions for Eqs. (13)–(19) are, for $r = 1$

$$\begin{aligned} & u = v = w = 0, \\ & B^r = \cos \alpha, \quad B^\alpha = -\sin \alpha, \quad B^\theta = B = \text{const.} \quad (20) \end{aligned}$$

The nondimensional parameters appearing in these equations are K , Ha , and Rm . The magnetic Reynolds number Rm is the ratio of the induced current to the net current.

Define a streamfunction for the secondary flow ψ as

$$u = \frac{1}{r} \frac{\partial \psi}{\partial \alpha}, \quad v = -\frac{\partial \psi}{\partial r},$$

and a magnetic potential A as

$$B^r = \frac{1}{r} \frac{\partial A}{\partial \alpha}, \quad B^\alpha = -\frac{\partial A}{\partial r}. \quad (21)$$

Equation (13) is satisfied and Eqs. (14)–(19), after substitution and cross differentiation of Eqs. (14) and (15) and elimination of the pressure, yield

$$\begin{aligned} & \nabla_1^2 w + C = (K/r)(\psi_\alpha w_r - \psi_r w_\alpha) \\ & + KN \{w[(B^r)^2 + (B^\alpha)^2]\}, \quad (22) \end{aligned}$$

$$\begin{aligned} & \frac{1}{K} \nabla_1^4 \psi + \frac{1}{r} \left(\psi_r \frac{\partial}{\partial \alpha} - \psi_\alpha \frac{\partial}{\partial r} \right) \nabla_1^2 \psi \\ & = -2w \left(\sin \alpha w_r + \frac{\cos \alpha}{r} w_\alpha \right) \\ & + N \left[\left(\frac{\partial}{\partial r} + \frac{1}{r} \right) (w B^\alpha B^\theta + \psi_r B' B') \right. \\ & + \frac{1}{r} \frac{\partial}{\partial r} (\psi_\alpha B' B^\alpha) \\ & \left. + \frac{1}{r} \frac{\partial}{\partial \alpha} \left(-w B' B^\theta + \psi_r B' B^\alpha + \frac{1}{r} \psi_\alpha B^\alpha B^\alpha \right) \right], \end{aligned} \quad (23)$$

$$\begin{aligned} & \left(\frac{1}{r} B^\alpha \psi_{\alpha\alpha} + \frac{1}{r} \psi_\alpha B^\alpha_\alpha + \psi_r B'_\alpha + B' \psi_{r\alpha} \right) \\ & + \frac{1}{\text{Km}} \left(\frac{\partial}{\partial \alpha} \nabla_1^2 A \right) = 0, \end{aligned} \quad (24)$$

$$\begin{aligned} & \left(-\frac{1}{r^2} B^\alpha \psi_\alpha + \frac{1}{r} B^\alpha \psi_{r\alpha} + \frac{1}{r} B'_r \psi_\alpha + B' \psi_{rr} + B'_r \psi_r \right) \\ & + \frac{1}{\text{Km}} \left(\frac{\partial}{\partial r} \nabla_1^2 A \right) = 0, \end{aligned} \quad (25)$$

$$\begin{aligned} & \frac{w}{r} B' + B' w_r + w B'_r + \frac{1}{r} (B^\alpha w_\alpha + w B^\alpha_\alpha) \\ & + \frac{1}{\text{Rm}} (\nabla_1^2 B^\theta) = 0, \end{aligned} \quad (26)$$

where

$$\nabla_1^2 \equiv \frac{\partial^2}{\partial r^2} + \frac{1}{r} \frac{\partial}{\partial r} + \frac{1}{r^2} \frac{\partial^2}{\partial \alpha^2},$$

and $N = \text{Ha}^2/K$ is the modified magnetic interaction parameter, $\text{Km} = \delta \text{Rm}$ and $C = G \text{Re}$. The boundary conditions at $r = 1$ are given by

$$w = 0, \quad \psi_r = 0, \quad \psi_\alpha = 0, \quad (27a)$$

$$A_\alpha = \cos \alpha, \quad A_r = \sin \alpha, \quad B^\theta = B = \text{const.} \quad (27b)$$

Equations (22)–(26), together with boundary conditions (27), describe completely the problem for the fully developed flow through a loosely coiled pipe.

III. SOLUTION

A. Low Hartmann number

In some fusion reactor applications [e.g., UWMAK-III (Ref. 2)], the magnetic Reynolds number, Rm , is very small [$\mathcal{O}(10^{-3})$]. For $\text{Rm} \ll 1$, Eqs. (24)–(26) may be approximated as

$$\nabla_1^2 A \simeq \text{const}, \quad (28)$$

$$\nabla_1^2 B^\theta \simeq 0. \quad (29)$$

With boundary conditions (27b), Eq. (28) will result in $A = r \sin \alpha$ which gives [see Eq. (21)] $B' = \cos \alpha$ and $B^\alpha = -\sin \alpha$. Equation (29), using the boundary condition (20), gives $B^\theta = B$. Substituting the above results in Eqs. (22) and (23), we get

$$\nabla_1^2 w + C = (K/r) (\psi_\alpha w_r - \psi_r w_\alpha) + KNw, \quad (30)$$

$$\begin{aligned} & \frac{1}{K} \nabla_1^4 \psi + \frac{1}{r} \left(\psi_r \frac{\partial}{\partial \alpha} - \psi_\alpha \frac{\partial}{\partial r} \right) \nabla_1^2 \psi \\ & = -2w [\sin \alpha w_r + (\cos \alpha/r) w_\alpha] \\ & + N \left[\left(\frac{\partial}{\partial r} + \frac{1}{r} \right) (\cos^2 \alpha \psi_r - B \sin \alpha w) \right. \\ & - \frac{1}{r} \frac{\partial}{\partial r} (\sin \alpha \cos \alpha \psi_\alpha) - \frac{1}{r} \frac{\partial}{\partial \alpha} \left(-B \cos \alpha w \right. \\ & \left. \left. - \sin \alpha \cos \alpha \psi_r + \frac{1}{r} \sin^2 \alpha \psi_\alpha \right) \right]. \end{aligned} \quad (31)$$

The above equations with boundary conditions (27a) can be solved for w and ψ .

Equations (30) and (31) have been solved numerically for the case of no magnetic field, $N = 0$, by McConalogue and Srivastava⁶ for small and intermediate values of the Dean number, and by Collins and Dennis⁷ for large Dean numbers.

For small values of the Dean number, Dean² solved analytically Eqs. (30) and (31) for the case of no magnetic field. He expanded the solution in a power series of the Dean number, i.e.,

$$w = \sum_{n=0}^{\infty} K^{2n} w_n(r, \alpha), \quad \psi = K \sum_{n=0}^{\infty} K^{2n} \psi_n(r, \alpha). \quad (32)$$

The objective of this work is to find an analytic solution for Eqs. (30) and (31), for small values of the Dean number. By doing so, the solution is expanded in a similar way to that seen in Eq. (32), but in two parameters K and N , i.e.,

$$w = w_{00} + \sum_{i=1}^{\infty} \sum_{j=0}^{\infty} K^i N^j w_{ij}, \quad (33)$$

$$\psi = \sum_{i=1}^{\infty} \sum_{j=0}^{\infty} K^i N^j \psi_{ij}. \quad (34)$$

Substituting the above series solutions in Eqs. (30) and (31) and equating the like power terms yield the weighting functions w_{ij} and ψ_{ij} , which are given in the Appendix.

The original Dean solution was expanded in the parameter K , defined as

$$K = 2\delta(\text{Re})^2.$$

The size of the coefficients in the Dean solution indicate that the series solution is valid for values of K up to $K = 576$.

The analytic solutions in the form of Eqs. (33) and (34) are even more restricted to the values of Ha of order unity. Thus this solution is not applicable in practical conditions where the Ha number is large (e.g., in magnetic fusion reactors). In the next section, we present another expansion which is valid in the intermediate Hartmann number range.

B. Intermediate Hartmann number

In the last section, the solution of the governing equations assumed a series solution defined by Eqs. (33) and (34). The zeroth order of this solution, w_{00} , is the axial velocity in a straight pipe, i.e., Poiseuille flow. The higher orders then show the effects of the curvature and magnetic body force. This solution, as mentioned above, is valid for the Hartmann number of order unity.

For the case of the intermediate Hartmann number, the

solution may be cast in a form in which the zeroth order reveals the flow in a straight pipe in a magnetic field. The effect of curvature will appear in higher-order solutions. These series solutions are defined as

$$w = w_0 + \sum_{j=1}^{\infty} K^j w_j, \quad (35)$$

$$\psi = \sum_{j=1}^{\infty} K^j \psi_j. \quad (36)$$

The governing equations [(30) and (31)] are written in a more convenient form:

$$\begin{aligned} (\nabla_1^2 - \text{Ha}^2)w &= -C + (K/r)(\psi_\alpha w_r - \psi_r w_\alpha), \\ \nabla_1^4 \psi + \frac{K}{r} \left(\psi_r \frac{\partial}{\partial \alpha} - \psi_\alpha \frac{\partial}{\partial r} \right) \nabla_1^2 \psi & \\ &= -2Kw [\sin \alpha w_r + (\cos \alpha/r)w_\alpha] \\ &+ \text{Ha}^2 \left[\left(\frac{\partial}{\partial \alpha} + \frac{1}{r} \right) (\psi_r B' B') + \frac{1}{r} \frac{\partial}{\partial r} (\psi_r B' B^\alpha) \right. \\ &\left. + \frac{1}{r} \frac{\partial}{\partial r} \left(\frac{1}{r} \psi_\alpha B^\alpha B^\alpha + \psi_r B' B' \right) \right]. \end{aligned}$$

Upon substituting the series solutions (35) and (36) into the above equations and equating the like power terms, the differential equation for the leading order solution is

$$(\nabla_1^2 - \text{Ha}^2)w_0 = -C,$$

which yields the zeroth-order solutions as

$$w_0 = \frac{C}{\text{Ha}^2} \left(1 - \frac{I_0(\text{Ha} r)}{I_0(\text{Ha})} \right),$$

where I_0 is the zeroth-order modified Bessel function.

The above solution for w_0 in the limit when $\text{Ha} \rightarrow 0$ is

$$w_0 = (C/4)(1 - r^2),$$

which is the Poiseuille flow solution. Here, w_0 is rescaled with respect to the mean velocity and written as

$$w_0 = \frac{I_0(\text{Ha}) - I_0(\text{Ha} r)}{I_0(\text{Ha}) - (2/\text{Ha})I_1(\text{Ha})}, \quad (37)$$

where I_1 is the first-order modified Bessel function. Calculations based on Eq. (37) give the zeroth-order velocity profile, which has the well established characteristics for MHD flow in straight ducts.

The higher-order solutions for the velocity and secondary flow streamline which reveal the curvature effects are

$$\psi_1 = P \sin \alpha \left(\sum_{k=0}^{\infty} (C_k^{(1)} - C_k^{(2)}) (\text{Ha} r)^{2k+1} \right), \quad (38)$$

and

$$\begin{aligned} w_2 &= \frac{P \cos \alpha}{I_0(\text{Ha}) - (2/\text{Ha})I_1(\text{Ha})} \sum_{k=1}^{\infty} (e_k^{(1)} - e_k^{(2)}) \\ &\times \left(\frac{\text{Ha}^{2k+1} I_1(\text{Ha} r)}{I_1(\text{Ha} r)} - (\text{Ha} r)^{2k+1} \right), \end{aligned} \quad (39)$$

where

$$P = 2 \text{Ha} [I_0(\text{Ha}) - (2/\text{Ha})I_1(\text{Ha})]^{-2},$$

$$b_k^{(1)} = \frac{I_0(\text{Ha})}{2^{2k+1} k!(k+1)!},$$

$$b_k^{(2)} = \sum_{l=0}^k \frac{1}{2^{2k+1} (l!)^2 (k-l)!(k-l+1)!},$$

$$C_0^{(j)} = \sum_{n=0}^{\infty} \frac{(n+1)b_n^{(j)}}{f(n)} \text{Ha}^{2n+4}, \quad j=1,2,$$

$$C_1^{(j)} = - \sum_{n=0}^{\infty} \frac{(n+2)b_n^{(j)}}{f(n)} \text{Ha}^{2n+2}, \quad j=1,2,$$

$$C_{k+2}^{(j)} = b_k^{(j)}/f(k), \quad j=1,2,$$

$$d_k^{(j)} = \sum_{l=0}^{\infty} \frac{C_l^{(j)}}{2^{2(k-l)+1} (k-l)!(k-l+1)!}, \quad j=1,2,$$

$$e_0^{(j)} = 0, \quad j=1,2,$$

$$e_{k+1}^{(j)} = \frac{d_k^{(j)} + e_k^{(j)}}{4(k+1)(k+2)}, \quad j=1,2,$$

$$f(k) = 192 + 448k + 368k^2 + 128k^3 + 16k^4.$$

IV. RESULTS AND CONCLUSIONS

The present analytical solution is valid over a limited range of parameters [up to $\text{Ha}^2 \sim \mathcal{O}(1000)$ and $\text{Rm} \sim \mathcal{O}(10^{-3})$]. However, in many fusion reactor applications, both the Hartmann and Reynolds magnetic numbers can exceed these limitations. The results presented in this section are indicative of expected behavior, particularly for the secondary flow, although numerical work may be required to extend the range of application.

The axial velocity contours for the low Hartmann number ($\text{Ha}^2 = 1$) and a Dean number ($K = 96$) are shown in Fig. 2(a). A relative convergence criterion of 10^{-3} was adopted to evaluate the velocity contours using the infinite series [Eqs. (38) and (39)]. The number of terms to achieve this criterion was found to be between 2 (low Hartmann numbers) and 20 (intermediate Hartmann numbers). The contours are nearly circular and are eccentric with their centers shifted toward the outer wall of the tube. The secondary flow streamlines for the same case are shown in Fig. 2(b). The results are very similar to Dean's solution,⁵ showing a small effect of the magnetic body forces on the nature of the secondary flow.

At intermediate values of the Hartmann number and the same Dean number, the axial velocity contours are distorted in a nonaxisymmetric fashion as shown in Fig. 3(a). The effect of the transverse magnetic field is to enhance the compression of fluid towards the outer wall. The conventionally symmetric Hartmann layer for fluid flow in a straight pipe is now quite asymmetric with respect to the pipe's toroidal center. Figure 3(b) shows the corresponding streamlines for the induced secondary flow at $\text{Ha}^2 = 1024$ and the same Dean number. It is interesting to note the effects of the magnetic field on the secondary flow field by comparing Figs. 2(b) and 3(b) when the same streamline contours are represented. The secondary flow field comprises the usual symmetric pair of counter-rotating vortices. The transverse magnetic field does not inhibit vortex formation, as one might intuitively think. One interesting effect of the magnetic field is that the flow streamlines are confined to a thin layer near the tube wall. The secondary flow rate in the near-wall boundary layer is increased by the magnetic field.

This phenomenon may have significant implications on convective heat transport in curved pipes used in the first walls and blankets of fusion reactors.

ACKNOWLEDGMENTS

This work was supported by the U.S. Department of Energy Contract No. DE-AA03-76SF80120 and the U. S. Department of Energy Office of Fusion Energy Grant No. DE-FG03-86ER52126, with UCLA.

APPENDIX: WEIGHTING FUNCTIONS

The approximate solutions for the velocity and secondary flow streamlines are in a series form [Eqs. (31) and (32)]. The weighting functions for these solutions, namely w_{ij} and ψ_{ij} , are listed below. All functions not listed below are equal to zero:

$$w_{00} = 1 - r^2, \quad (\text{A1})$$

$$w_{20} = (\cos \alpha / 2^8 \cdot 45) f_2, \quad (\text{A2})$$

$$w_{40} = 1 / (2^{18} \cdot 3^6 \cdot 5^2 \cdot 7^2) (\cos^2 \alpha f_{34} + \sin^2 \alpha f_{35}), \quad (\text{A3})$$

$$w_{11} = \frac{1}{16} (-3 + 4r^2 - r^4), \quad (\text{A4})$$

$$w_{21} = (B \cos \alpha / 48^2) f_5, \quad (\text{A5})$$

$$w_{31} = 1 / (2^{13} \cdot 3^3 \cdot 5^2 \cdot 7) (14 f_9 \cos \alpha + f_{10} \cos^3 \alpha + f_{11} \sin^2 \alpha \cos \alpha), \quad (\text{A6})$$

$$w_{22} = \frac{1}{376} f_{13}, \quad (\text{A7})$$

$$w_{32} = B / (2^{14} \cdot 3^3 \cdot 5^2) (40 f_{17} \cos \alpha + f_{18} \cos^3 \alpha + f_{19} \sin^2 \alpha \cos \alpha), \quad (\text{A8})$$

$$w_{33} = 1 / (2^{19} \cdot 9) f_{27}, \quad (\text{A9})$$

$$\psi_{10} = (\sin \alpha / 288) f_1, \quad (\text{A10})$$

$$\psi_{30} = (\sin \alpha \cos \alpha) / (2^{14} \cdot 3^4 \cdot 5^2 \cdot 7) f_3, \quad (\text{A11})$$

$$\psi_{11} = (B \sin \alpha / 96) f_4, \quad (\text{A12})$$

$$\psi_{21} = \frac{\sin \alpha}{2^{10} \cdot 45} f_6 + \frac{1}{2^{11} \cdot 3^3 \cdot 5} \times (f_7 \sin \alpha \cos^2 \alpha + f_8 \sin^3 \alpha), \quad (\text{A13})$$

$$\psi_{31} = (B \sin \alpha \cos \alpha) / (2^{13} \cdot 3^4 \cdot 5^2 \cdot 7) f_{12}, \quad (\text{A14})$$

$$\psi_{22} = B / (2^{10} \cdot 45) (10 f_{14} \sin \alpha$$

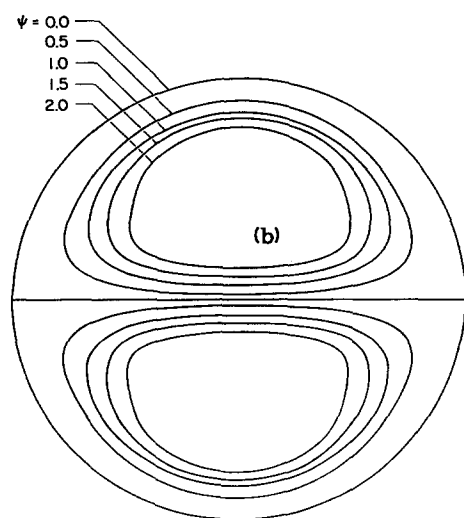
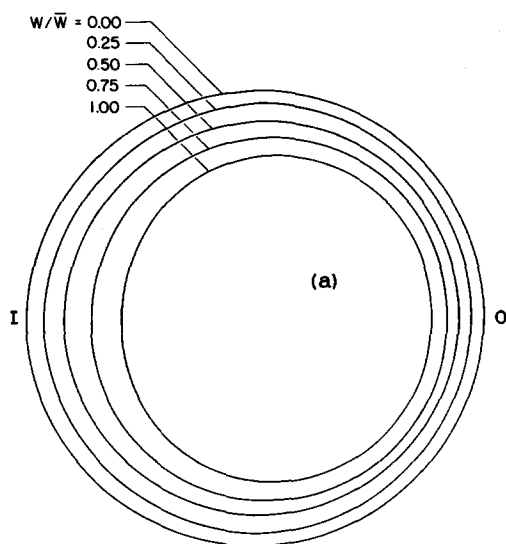


FIG. 2. (a) Axial velocity contours and (b) secondary flow streamlines, for the low Hartmann number ($Ha^2 = 1$).

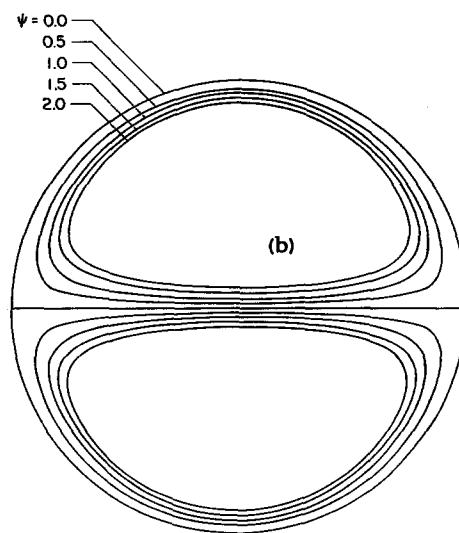
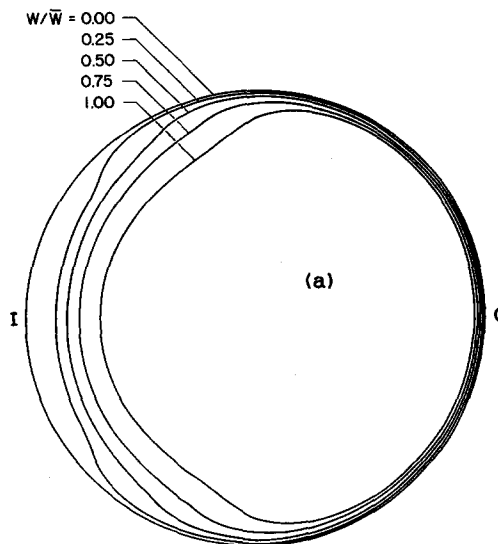


FIG. 3. (a) Axial velocity contours and (b) secondary flow streamlines, for the intermediate Hartmann number ($Ha^2 = 1024$).

$$+f_{15} \sin \alpha \cos^2 \alpha + f_{16} \sin^3 \alpha), \quad (\text{A15})$$

$$\psi_{32} = \frac{\sin \alpha}{2^{12} \cdot 3^3 \cdot 5^2} f_{20} + \frac{B^2 \sin \alpha \cos \alpha}{2^{14} \cdot 3^3 \cdot 5} f_{21}$$

$$+ \frac{1}{2^{14} \cdot 3^3 \cdot 5^2 \cdot 7} (f_{22} \sin \alpha \cos^2 \alpha + f_{23} \sin^3 \alpha)$$

$$+ \frac{1}{2^{17} \cdot 3^3 \cdot 5^2 \cdot 7} (f_{24} \sin \alpha \cos^4 \alpha$$

$$+ f_{25} \sin^3 \alpha \cos^2 \alpha + f_{26} \sin^5 \alpha), \quad (\text{A16})$$

$$\psi_{33} = \frac{B \sin \alpha}{2^{13} \cdot 45} f_{28} + \frac{B}{2^{15} \cdot 3^3 \cdot 5}$$

$$\times (f_{29} \sin \alpha \cos^2 \alpha + f_{30} \sin^3 \alpha)$$

$$+ \frac{B}{2^{16} \cdot 3^3 \cdot 5^2 \cdot 7} (f_{31} \sin \alpha \cos^4 \alpha$$

$$+ f_{32} \sin^3 \alpha \cos^2 \alpha + f_{33} \sin^5 \alpha), \quad (\text{A17})$$

where $f_i(r)$ functions are

$$f_1 = 4r - 9r^3 + 6r^5 - r^7, \quad (\text{A18})$$

$$f_2 = 19r - 40r^3 + 30r^5 - 10r^7 + r^9, \quad (\text{A19})$$

$$f_3 = 4979r^2 - 12\,750r^4 + 11\,340r^6 - 4480r^8$$

$$+ 1050r^{10} - 144r^{12} + 5r^{14}, \quad (\text{A20})$$

$$f_4 = r - 2r^3 + r^5, \quad (\text{A21})$$

$$f_5 = 3r - 6r^3 + 4r^5 - r^7, \quad (\text{A22})$$

$$f_6 = -247r + 576r^3 - 420r^5 + 100r^7 - 9r^9, \quad (\text{A23})$$

$$f_7 = -39r + 144r^3 - 180r^5 + 84r^7 - 9r^9, \quad (\text{A24})$$

$$f_8 = -39r + 88r^3 - 60r^5 + 12r^7 - r^9, \quad (\text{A25})$$

$$f_9 = -3056r + 6675r^3 - 5480r^5 + 2250r^7$$

$$- 420r^9 + 31r^{11}, \quad (\text{A26})$$

$$f_{10} = -602r + 1665r^3 - 1925r^5 + 1155r^7$$

$$- 315r^9 + 22r^{11}, \quad (\text{A27})$$

$$f_{11} = -602r + 465r^3 + 1015r^5 - 1365r^7$$

$$+ 525r^9 - 38r^{11}, \quad (\text{A28})$$

$$f_{12} = 3111r^2 - 7450r^4 + 5775r^6$$

$$- 1680r^8 + 280r^{10} - 36r^{12}, \quad (\text{A29})$$

$$f_{13} = 19 - 27r^2 + 9r^4 - r^6, \quad (\text{A30})$$

$$f_{14} = -10r + 21r^3 - 12r^5 + r^7, \quad (\text{A31})$$

$$f_{15} = -5r + 17r^3 - 19r^5 + 7r^7, \quad (\text{A32})$$

$$f_{16} = -5r + 11r^3 - 7r^5 + r^7, \quad (\text{A33})$$

$$f_{17} = -178r + 375r^3 - 285r^5 + 100r^7 - 12r^9,$$

$$(\text{A34})$$

$$f_{18} = -135r + 357r^3 - 385r^5 + 208r^7 - 45r^9,$$

$$(\text{A35})$$

$$f_{19} = -135r + 129r^3 + 155r^5 - 224r^7 + 75r^9,$$

$$(\text{A36})$$

$$f_{20} = 4037r - 9580r^3 + 7300r^5 - 2025r^7$$

$$+ 285r^9 - 17r^{11}, \quad (\text{A37})$$

$$f_{21} = 17r^2 - 36r^4 + 20r^6 - r^{10}, \quad (\text{A38})$$

$$f_{22} = 4179r - 15\,795r^3 + 20\,430r^5 - 10\,290r^7$$

$$+ 1575r^9 - 99r^{11}, \quad (\text{A39})$$

$$f_{23} = 4179r - 9505r^3 + 6630r^5 - 1470r^7$$

$$+ 175r^9 - 9r^{11}, \quad (\text{A40})$$

$$f_{24} = 1008r - 5170r^3 + 9010r^5 - 6685r^7$$

$$+ 1980r^9 - 143r^{11}, \quad (\text{A41})$$

$$f_{25} = 2016r - 7460r^3 + 9820r^5 - 5390r^7$$

$$+ 1080r^9 - 66r^{11}, \quad (\text{A42})$$

$$f_{26} = 1008r - 2290r^3 + 1610r^5 - 385r^7 + 60r^9 - 3r^{11},$$

$$(\text{A43})$$

$$f_{27} = -211 + 304r^2 - 108r^4 + 16r^6 - r^8, \quad (\text{A44})$$

$$f_{28} = 143r - 304r^3 + 180r^5 - 20r^7 + r^9, \quad (\text{A45})$$

$$f_{29} = 99r - 348r^3 + 408r^5 - 168r^7 + 9r^9, \quad (\text{A46})$$

$$f_{30} = 99r - 220r^3 + 144r^5 - 24r^7 + r^9, \quad (\text{A47})$$

$$f_{31} = 385r - 1876r^3 + 3092r^5 - 2096r^7 + 495r^9,$$

$$(\text{A48})$$

$$f_{32} = 770r - 2744r^3 + 3448r^5 - 1744r^7 + 270r^9,$$

$$(\text{A49})$$

$$f_{33} = 385r - 868r^3 + 596r^5 - 128r^7 + 15r^9, \quad (\text{A50})$$

$$f_{34} = -259\,497 + 1\,632\,020r^2 - 3\,691\,212r^4$$

$$+ 4\,322\,430r^6 - 2\,999\,682r^8 + 1\,287\,132r^{10}$$

$$- 344\,908r^{12} + 46\,242r^{14} - 2525r^{16}, \quad (\text{A51})$$

$$f_{35} = -259\,497 + 1\,049\,260r^2 - 2\,147\,628r^4$$

$$+ 2\,663\,010r^6 - 2\,018\,898r^8 + 928\,452r^{10}$$

$$- 247\,212r^{12} + 34\,398r^{14} - 1885r^{16}. \quad (\text{A52})$$

¹J. Hartmann, K. Dan. Vidensk. Selsk. Mat.-Fys. Medd. **15**, 1 (1937).

²G. Yagawa and M. Masuda, Nucl. Eng. Des. **71**, 121 (1982).

³J. P. Blanchard and N. M. Ghoniem, Nucl. Eng. Des. **2**, 19 (1985).

⁴S. A. Berger, L. Talbot, and L. S. Yao, Annu. Rev. Fluid Mech. **15**, 461 (1983).

⁵W. R. Dean, Philos. Mag. **30**, 673 (1928).

⁶D. J. McConalogue and R. S. Srivastava, Proc. R. Soc. London Ser. A **307**, 37 (1968).

⁷W. M. Collins and S. C. R. Dennis, Q. J. Mech. Appl. Math. **28**, 133 (1975).

⁸J. A. Shercliff, J. Fluid Mech. **1**, 644 (1956).

⁹C. C. Chang and T. S. Lundgren, Z. Angew. Math. Phys. **12**, 100 (1961).

¹⁰R. J. Holroyd and J. S. Walker, J. Fluid Mech. **84**, 471 (1978).

¹¹J. S. Walker, J. Fluid Mech. **167**, 199 (1986).

¹²H. Branover, *Magnetohydrodynamic Flow in Ducts* (Wiley, New York, 1978).